atmospheric short-term instability. These are much larger than the DIMM uncertainty given by the vertical error bars (statistical error $< \pm 5\,\%$).

DIMM 3 was first used to check the comparability of its two predecessors before being transported to the newly equipped summit of **Cerro la Montura,** 2509 m, 4 km north-east of Paranal, shown on Figure 2. Contrary to Vizcachas and La Silla, those two northern summits present very different wind patterns. This has raised some concern that the lower wind velocity found at La Montura might be traded against an increase of local seeing. Regular measurements started there on April 1 to detect possible differences with the nearby Paranal.

References

1. H. Pedersen et al.: Seeing Measurements with a Differential Image Motion Monitor; *The Messenger* No. 53; September 1988, 8–9.
2. M. Sarazin, F. Roddier: The ESO differential image motion monitor; submitted to *Astron. Astroph.*, Feb. 1989.

The VLT in the Wind Tunnel

L. ZAGO, ESO

Introduction

Increasing evidence collected over recent years has shown that the best local seeing conditions are found when the telescope is exposed to an undisturbed moderate wind flow. This recognition has contributed decisively to direct the design of new telescope buildings towards more open and, incidentally, cheaper solutions than the conventional domes.

The unit telescopes of the VLT are being designed for operation in the open air with a fully openable inflatable dome at present considered for daytime protection. With this concept the wind becomes an important loading condition in the design of the telescope and its effects must be quantified accurately. In order to provide the required data, a series of wind tunnel tests has been performed with models of the VLT unit telescope and its enclosure.

Wind Tunnel Simulation

The basic problem of tests at a reduced scale is that it is seldom possible to scale down all intervening quantities. This is also true for wind tunnel tests where, for instance, it is obviously not possible to scale down the air molecules and gravity. One has to identify the main factors which determine the amplitude of the aerodynamic force for each particular case, then try to simulate those factors as accurately as possible and estimate the corrections due to other parameters which cannot be simulated rigorously.

The aerodynamic force applied on an object is conventionally defined as:

$$F = \frac{1}{2} C_p S \varrho V^2 \qquad (1)$$

with V the flow velocity, ϱ the air density, S a reference surface (generally the exposed cross-section) and C_p an adimensional coefficient mainly dependent on the object shape, but also on the relationship of some flow characteristics to the scale of the object.

In general, the largest part of the aerodynamic force applied on an object depends on the size, number and type of the vortices generated in the wake. For low velocity flows such as atmospheric wind, this wake turbulence, hence C_p, is mainly affected by two parameters: the turbulence already present in the upstream flow and the Reynolds number, which expresses the product of geometry and velocity scales, relative to viscosity.

The first consequence is that, since the atmospheric boundary layer is turbulent, this turbulence must be reproduced in the wind tunnel upstream of the model. This requires special installations, properly called boundary layer wind tunnels, which have a rectangular cross-section and a length sufficient to build up a scaled down atmospheric turbulence upstream of the test model. Even in such wind tunnels, however, it is not possible to achieve a complete Reynolds number similarity: this would require that velocity be increased by the same factor as the geometry scale is reduced, which in many cases would make the flow supersonic. Nonetheless, the C_p of sharp-edged objects is not too dependent on the Reynolds number, so that the measurements are generally accurate enough for most purposes in building engineering, where the objective mostly concerns the determination of ultimate dimensioning loads, to which some safety margin is anyway added.

In the VLT case, the determination of wind loading is required to quantify the "normal" performance of the telescope, hence a greater accuracy is desired than the one achievable in standard tests. Furthermore, the telescope structure is made of round section members, which have a low drag but also a C_p which is quite dependent on the Reynolds number. Therefore, the wind tunnel test measurements on the VLT model had to be complemented and corrected by separate tests of telescope bar elements at both full and model scale. The measurements were then used to calibrate and validate a detailed numerical model of the telescope. In this way, not only the full scale loads on the telescope were evaluated with better accuracy than otherwise achievable, but also further possible design changes of the telescope structure will not need new tests, but just a new run of the numerical model with updated inputs.

Some Results

While it is not the purpose of this article to present all the results of the VLT wind tunnel tests, below are a few examples which illustrate some interesting aspects of this work.

The scale of the VLT model was 1 : 80. Two different enclosure configurations were tested in the wind tunnel, both of which assume an inflatable dome fully open during observations. The first enclosure surrounds the tele-

(a)

(b)

Figure 1: *Some of the configurations tested in the wind tunnel: (a) Telescope imbedded in a recess platform. (b) Open platform with the telescope exposed.*

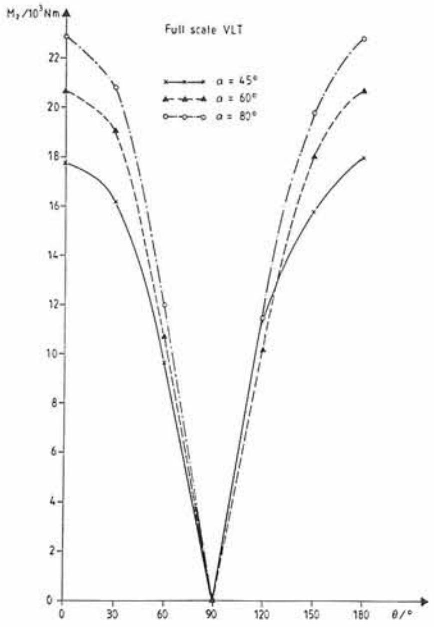

Figure 2: *Full scale altitude torque for the telescope imbedded in the recess platform as function of azimuth angle θ for elevation angles α = 45°, 60° and 80°, with a mean wind speed of 16 m/s.*

scope approximately up to the level of the altitude axis, with the lower part imbedded in a recess. This is at present the preferred solution as it allows control of the wind loading on the primary mirror. The second configuration leaves the telescope fully exposed to the wind and was previously envisaged in conjunction with a linear wind screen, which was also simulated in the wind tunnel.

Static Wind Loading

The most important result concerning static wind loading is the torque about the altitude axis (Fig. 2), which is a main parameter for the design of the drives. The torque about the azimuth axis is, in the worst case, only about half the previous one.

Flow in the Platform Recess

Some tests have provided evidence for a recirculation pattern inside the platform recess (Figs. 3 and 4). This may be very useful in order to ensure a moderate ventilation around the primary mirror. In any case, the final enclosure design will include doors and semi-permeable wind screens integrated in the recess wall which will allow alteration of the flow pattern in order to achieve anything between a very still environment and natural ventilation with ambient air.

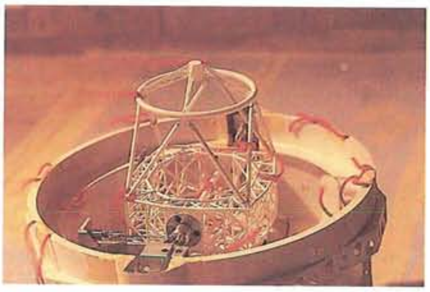

Figure 3: *Flow visualization with wool tufts showing the recirculation pattern in the recess.*

Wind Loading on the Primary Mirror

The wind loading on the primary mirror was measured by means of 32 tiny pressure tubes, which allowed accurate mapping of the distribution of pressure coefficients.

Dynamic Wind Loading

This was one of the most interesting parts of the tests for its implications on the further design of the telescope control systems. In general, the dynamic wind loading can be determined by means of expression (1), considering the wind velocity term as a function of time V(t). Thus the coefficients determined from the static loading measurements can also be used in a dynamic response analysis.

Moreover, two additional parameters are required. The first one is the actual spectral distribution of wind energy on the telescope. The objective of some wind tunnel measurements was indeed to determine the influence of the different enclosure types, since "natural" wind spectra have already been measured on the possible VLT sites. The second dynamic parameter is the aerodynamic admittance of the structure, which quantifies the filtering effect of a large structure with respect to high frequency fluctuations.

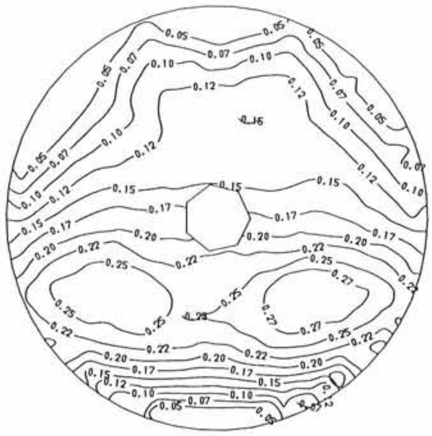

Figure 5: *Contour map of pressure coefficients on the primary mirror for 0° azimuth and 60° elevation. In this case the local pressure coefficients vary between 0.05 and 0.27.*

Acknowledgements

The VLT wind tunnel tests were performed by the Ecole Polytechnique Fédérale of Lausanne, Switzerland, under ESO contract. Special acknowledgement is accorded to the personal contributions of J.-A. Hertig and C. Alexandrou.

References

[1] Zago L.: Latest Studies Lead to Revised Design of the VLT Enclosure, *The Messenger*, No. 52, p. 7.

[2] Hertig J.-A., Alexandrou C., and Zago L.: Wind tunnel tests for the ESO VLT, Proc. ESO Conf. on Very Large Telescopes and their Instrumentation, pp. 867–876, Garching, March 1988.

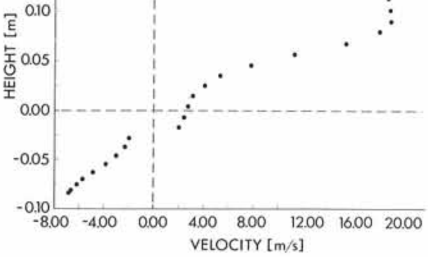

Figure 4: *Mean velocity profile measured just in front of the telescope tube (set vertical). Note that the height is given in the model 1 : 80 scale.*

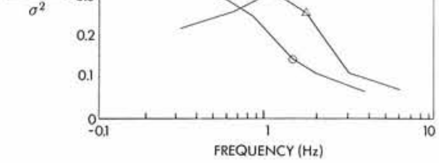

Figure 6: *Wind velocity spectrum measured just in front of the telescope tube B), compared with the one measured at the same location in the empty wind tunnel A). The difference of the two spectra quantifies the turbulence generated by the platform.*